(2)

FASTC-ID(RS)T-1065-91

FOREIGN AEROSPACE SCIENCE AND TECHNOLOGY CENTER

A SIMULATION STUDY OF PLANAR SWAGING DEFORMATION

by

Cheng-Gen Zhang, Gwang-Shen Jen, Gwang-Huei Su

HUMAN TRANSLATION

FASTC-ID(RS)T-1065-91 28 August 1992

A SIMULATION STUDY OF PLANAR SWAGING DEFORMATION

By: Cheng-Gen Zhang, Gwang-Shen Jen, Gwang-Huei Su

English pages: 16

Source: Jixie Gongcheng Xuebao, Vol. 25, Nr. 3, September 1989; pp. 72-77

Country of origin: China
Translated by: SCITRAN
F33657-84-D-0165
Requester: WL/MLLM/Henrich
Approved for public release; Distribution unlimited.

PREPARED BY:

TRANSLATION DIVISION
FOREIGN AEROSPACE SCIENCE AND TECHNOLOGY CENTER
WPAFB, OHIO

GRAPHICS DISCLAIMER

All figures, graphics, tables, equations, etc. merged into this translation were extracted from the best quality copy available.

A Simulation Study of Planer Swaging Deformation

Zhang, Cheng-Gen; Jen, Gwang-Shen
(Ji-Lin Industrial University)

Su, Gwang-Huei
(Beijing Mechanical and Electrical Research Institute, Ministry of Mechanical and Electrical Industries)

Abstract Planer swaging deformation was studied with photoplastic method. The domestic polycarbonate was used as a simulation material. The full-field strain distribution for planer swaging deformation was obtained. The average error of the calculated strain was less than 7%. The deformation area and the effect of friction on deformation area were studied with the characteristics of photoplasticity. This paper points out the special features of planer swaging deformation and the effect of lubrication on deformation flow.

key words: planer swaging, deformation, photoplasticity

(Manuscript received in December, 1987. Revised paper received in January, 1988.)

I. Introduction

Planer swaging is a typical two-dimensional plastic deformation. It is also the most basic swaging practice and the fundamental for the theoretical analysis of two-dimensional plastic deformation. In the study of swaging deformation, a more frequently adopted method is the visual plastic method. The

pattern of material flow and the effect of technical parameters on deformation are analyzed through the deformation of grids on the samples. Even though this method provide a direct analytical method, its quantitative accuracy was somewhat poor.

Recently, Moire pattern and photoplasticity methods were included in the study of plastic deformation and the accuracy of quantitative plastic deformation was improved. Moire pattern method utilizes the photomechanics of the light-sensitive thin film which deforms with the bulk body to simulate deformation and is mainly used in two-dimensional deformation study. Photoplastic method utilizes the photodynamical properties of light-sensitive materials with the similar deformation properties as the metallic materials to study the force and deformation in plastic flow. Hence, photoplastic method can be used not only in the study of two-dimensional problems, it can also provide information regarding three-dimensional full-field strain distribution. The force and strain along any direction of any point in the body can be obtained. Therefore, photoplastic method serves as a highly effective method in the analysis of plastic deformation.

The study of photoplasticity became important since the 50's. Earlier studies mainly focused on the stress components during plastic deformation.[1] Accompanied by the introduction of new simulation materials in the 70's,[2,3] the study of plastic strain was initiated. Presently, the major study topic is the deformations along the direction of principle stresses.[4,5] The relative magnitude of the various strain components can be determined through theoretical analysis and, therefore, the

experimental procedures were relatively easy and the solution can be obtained quickly. However, directions of most of the principle strains in plastic deformation are unknown. Because of this difficulty with other techniques, the photoplastic method, which provides the solution for deformation problems without the requirement of knowledge of directions of principle strains, and its experimental technique become even more important.

II. Principles of Photoplastic Experiment

The technique of photoplastic method was developed based on the foundation of photoelastic method. Due to the effect of double-refraction, in the polarized light field, of plastically deformed light sensitive materials, the force and deformation during plastic deformation can be studied by simulation.

As one research showed[1] that plastic deformation occurs in some of the light-sensitive materials which solidify, on the molecular level, in the materials. The double-refraction pattern due to plastic deformation can be related to the strain during plastic deformation by

$$\bar{\delta} = f(\varepsilon_i, \sigma_i, h) \qquad i = 1, 2, 3 \qquad (1)$$

where δ is difference in light traveling distance and h is the thickness of the test sample.

Further analysis showed[2] that for some materials, such as polycarbonate, a linear relationship exists, in the range of plastic deformation, between the double-refraction pattern and principle strain. The strain-optical principle of plastic deformation of this type can be expressed as:

$$\varepsilon_1 - \varepsilon_2 = \frac{f \cdot N}{h} \qquad (2)$$

where f is the number of material strain lines and N is the order of the lines.

For any point of the deformed body, if observation is made along the three coordinate axes under polarized light, the corresponding line order N and the angle between the principle strain and coordinate axes θ can be obtained. Therefore, for each coordinate axis, the strain-optical equations can be established. For example, for the plane perpendicular to z axis,

$$\varepsilon_x - \varepsilon_y = (\varepsilon_1 - \varepsilon_2)\cos 2\theta_z = \frac{N_z f}{h_z} \cdot \cos 2\theta_z \qquad (3)$$

$$\gamma_{xy} = \frac{1}{2}(\varepsilon_1 - \varepsilon_2) \cdot \sin 2\theta_z = \frac{N_z \cdot f}{2h_z} \cdot \sin 2\theta_z \qquad (4)$$

Similarly, the equations for the other two coordinate axes are:

$$\varepsilon_y - \varepsilon_z = \frac{N_x \cdot f}{h_x} \cdot \cos 2\theta_x \qquad (5)$$

$$\gamma_{yz} = \frac{N_x \cdot f}{2h_x} \cdot \sin 2\theta_x \qquad (6)$$

$$\varepsilon_z - \varepsilon_x = \frac{N_y \cdot f}{h_y} \cdot \cos 2\theta_y \qquad (7)$$

$$\gamma_{zx} = \frac{N_y \cdot f}{2h_y} \sin 2\theta_y \qquad (8)$$

There are only five independent equations in eq.(3) to eq.(8) and one more equation is needed in order to have a

solution. The condition of non-compressibility is satisfied in plastic deformation and

$$\varepsilon_1 + \varepsilon_2 + \varepsilon_3 = \varepsilon_x + \varepsilon_y + \varepsilon_z = 0 \qquad (9)$$

Combining equations (4) to (9), the strain at one point of the deformed body can be solved.

For two-dimensional deformation and axial symmetric deformation, the solution can be obtained with the two equations of one coordinate axis and the requirement of non-compressibility.

The study of domestic polycarbonate showed[6,7] that the poison's ratio of polycarbonate during plastic deformation is 0.5. Because the properties of plastic deformation of polycarbonate are similar to those of thermal deformation of metals, polycarbonate can be used as the material for photoplastic study.

The study of strain-line pattern showed that the strain lines of polycarbonate under high-voltage mercury lamp is: f_e=0.0018mm/line.

Because of the superior machining characteristics and plastic deformation properties of polycarbonate, deformation can take place under constant temperature in modular dies. Since there is no special requirements about experimental technique, polycarbonate can be used conveniently in the study of plastic deformation.

III. Experimental Study and Analysis of Result

The experiment of planer swaging was performed in assembled modular dies. When swaging has gone to certain level, the modular dies can be disassembled and the samples can be taken out. The dies were designed based on a swaging ratio of 2. Different swaging ratio can be obtained by adding pads or gaskets in the chamber of the modules. Also, different swaging angles are available by using different swaging wedges. In this study, the swaging deformations with swaging angles of 30^{o}, 45^{o}, and 60^{o} and swaging ratios of 1.5 and 2 were studied.

The samples used in planer swaging experiment are rectangular samples, with one end machined to conform to the shape of die chamber and serves as the conducting end. The sample dimension was $40x20x60mm^3$ when the swaging ratio was 2. The surfaces of the swaging samples were polished and silicon grease was used for lubrication during swaging operation. Therefore, the planer swaging experiment can be viewed as the ideal frictionless operation.

A thin slice was taken from the swaged sample for photoplastic analysis. Because of the high optical sensitivity of polycarbonate material, the line density of plastically deformed sample is high. It is based on this concern that the slices used for photoplastic analysis are generally very thin, on the order of 0.5 to 1 mm.

The prepared slices were placed in polarized light field and the deformation optical effect provided the information of planer swaging deformation. The results are summarized as follows:

1. Deformation Area Range of Planer Swaging

The deformation area range of planer swaging is one of the major parameters of the analysis of planer swaging deformation. The range of deformed area determines the type of deformation and the plotting of sliding line.

For plastically deformed polycarbonate, the significant increase in the line density defines the boundary of elastic/plastic deformation; namely, the upper limit of deformation area as shown in the top and central portions of figure 1. The lower limit of the deformation area can be determined by the characteristics of the equislope lines. Equislope line is the trace of points with identical principle strain directions and all the points on one given equislope line have the same principle strain directions. During planer swaging, the directions of principle strains of the deforming portion are constantly changing while the directions of principle strains of deformed portion are identical - the protruding directions. Therefore, the equislope lines of the deformed portion have the same tilting degrees. The equislope lines of the bottom dark area of figure 1 have 0 degrees of tilting angle, which shows that the directions of the principle strains are along the protruding directions. The boundary between the 0 degrees equislope lines and the deforming portion is the lower limit of the deformation area. The portion between the upper and lower limits of the deformation area is the deformed area of planer swaging.

2. The Effect of Friction on the Deformation Area

Fig. 1: The 0 degree equislope lines which determines the planer swaging deformation area

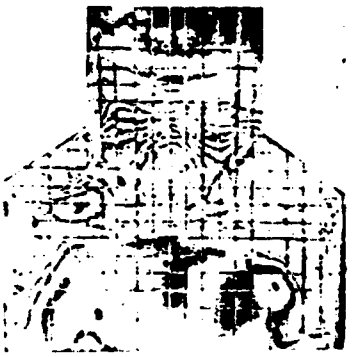

Fig. 2: Die wall adherence equivariance line pattern

The deformation area of planer swaging is determined by modular die parameters and friction condition. Different friction condition result in different deformation area.

To study the effect of friction on swaging deformation some of the samples were not thoroughly lubricated when swaged and certain friction existed during swaging operation. Friction causes variation in the deformation area. Figure 2 shows the equivariance line pattern when adherence friction occurs along the surface of the sample.

Because of the adherence friction between the walls of the die and the swaged part, the triangular shaped adherence non-deforming region formed before entering the swaging wedge as shown in the corner of figure 2 where the line density is low. Deformation occurs from this adherence region up. The existence of the adherence region pushes the deformation region forward, enlarges the deformation area, increases the deformation force, and shortens the serviceable life of die. Because of the localized high plastic flow due to adherence region, the deformation flow becomes unreasonable and the quality of the product is deteriorated.

IV. Determination of Full Field Strain and Error Analysis

For planer swaging deformation, because $e_z=0$, equation (9) can be re-written as

$$\varepsilon_x + \varepsilon_y = 0 \qquad (10)$$

Combining equations (3) and (10) one would have

$$\varepsilon_x = -\varepsilon_y = \frac{N_x \cdot f}{2h_x}\cos 2\theta_x \qquad (11)$$

From the order of equivariance line N and degree of equislope line θ provided by the photoplastic analysis and the boundary conditions, the strain state of any point can be solved from equations (11) and (4).

Because the N and θ can be measured for any corresponding point of the sample, the strain state of any point of the deformed region can be solved. In order to obtain the full field strain distribution, the 2x2 grid was plotted on the sample surface and the N and θ of each grid point were measured for the calculation of the strain state of each grid point. The full field strain distribution is then constructed from the strain state of each grid point. The strain distribution was actually calculated and plotted with the numerical processing capability of a computer. The strain distribution for the case of swaging ratio of 2 and swaging angle of 45^{o} was used as an example. Figure 3 shows the distribution of normal strain, figure 4 shows the distribution of shear strain, and figure 5 shows the distribution of normal strain and shear strain parallel to the cross section of the x-axis and the numerical values of the maximum normal strain and maximum shear strain.

It can be learned that: the normal strain distribution on the cross section is symmetrical while the shear strain distribution is asymmetrical. This illustrates that the planer swaging deformation is symmetrical with respect to y axis. The strain e_y on the cross section parallel to x-axis in the deformed region composes of tensile and compressive deformation regions.

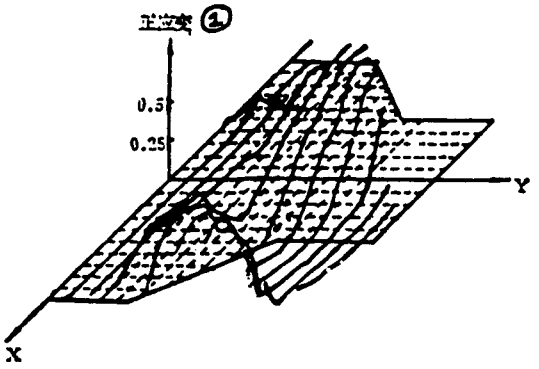

key: 1 - normal strain

Fig. 3: Y axis normal strain distribution

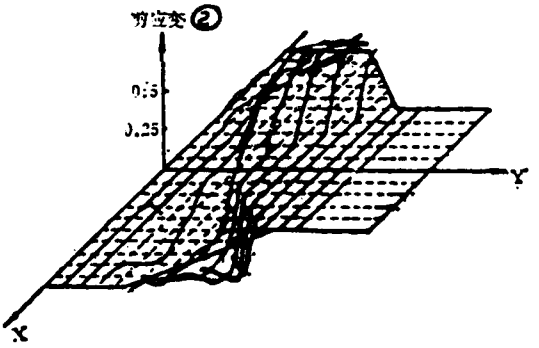

key: 2 - shear strain

Fig. 4: Shear strain distribution

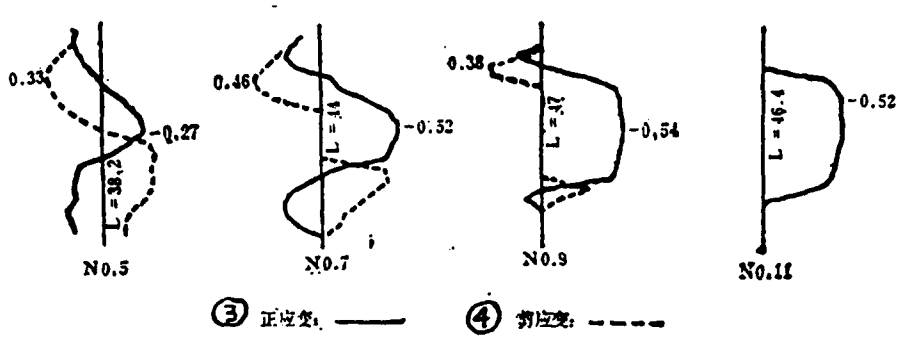

key: 3 - normal strain

4 - shear strain

Fig. 5: Distribution of some of the strains parallel to the x-axis cross section

The e_y of the central region is tensile deformation region while the two sides are the compressive deformation regions.

Since

$$e_y = -e_x = -\frac{Nf_s}{2h} \cdot \cos 2\theta \quad \text{Ⓐ}$$

when $e_y > 0$, $\cos 2\theta < 0$, $\theta > 45^\circ$

when $e_y < 0$, $\cos 2\theta > 0$, $\theta < 45^\circ$

and the variation of the tensile stress of the normal strain can be delineated by the 45° equislope lines.

In order to determine the accuracy of the calculated result, the strain distribution and the width after deformation were used to calculate the width before deformation which was compared with the actual width.

From the definition of strain,

$$\varepsilon = \frac{\Delta l}{l} = \frac{l' - l}{l'} \quad \text{Ⓑ}$$

$$l' = \frac{l}{1 - \varepsilon} \quad \text{Ⓒ}$$

where l is the width before deformation and l' is the width after deformation.

The width between two adjacent grid points j and j+1, before deformation, is

$$l'_{j,j+1} = \frac{l_{j,j+1}}{1 - \bar{\varepsilon}_{j,j+1}} \qquad (12)$$

where $l_{j,j+1}$ is the distance between two grid points

$$\bar{\varepsilon}_{j,j+1} = \frac{1}{2}(\varepsilon_j + \varepsilon_{j+1}) \quad \text{Ⓓ}$$

The width of the test sample before deformation can be obtained by summation of the widths, before deformation, of

successive adjacent grid points. Figure 5 shows the calculated widths of some of the cross sections before deformation. The maximum error was 17.5% and the average error was 7%. Major causes of these errors were related to sample fabrication and measurement accuracy.

The size of the deformation region and effect of various deformation parameters on the swaging deformation can be determined by the magnitude of the equivalent strain. The two-dimensional equivalent strain at any point can be expressed by equation (13)

$$\bar{\varepsilon} = \frac{2}{3}\left[(\varepsilon_x - \varepsilon_y)^2 + \varepsilon_x^2 + \varepsilon_y^2 + 6\varepsilon_{xy}^2\right]^{\frac{1}{2}} \qquad (13)$$

For the swaging deformation with swaging ratio of 2 and swaging angle of 45°, the maximum equivalent strain occurs below the cross point of the two fan-shaped deformation regions along the central symmetrical axes. The maximum equivalent strain $\bar{\varepsilon}_{45}$ is 0.54.

The full-field strain distribution of planer swaging operation obtained by photoplastic method provides a set of quantitative strain data of planer swaging deformation. The accuracy provided by this method can be applied in actual engineering practices.

V. Conclusions

(1) The deformation region of planer swaging operation can be determined by photoplastic method.

(2) The shape of deformed area is strongly affected by the friction condition. Different friction condition results in different deformation flow mode and the friction between the die surface and the test sample further complicates the shape of deformation region.

(3) The accuracy of full field strain distribution determined by the photoplastic method can be applied in actual engineering practices. There are tensile deformation as well as compressive deformation on the same cross section and their boundaries can be determined by equislope lines.

(4) The photoplastic analytic method described in this paper can be applied in other analyses of plastic deformation.

BIBLIOGRAPHY

1. Javournicky J: Photoplasticity, New York: Esevier Scientific Publishing Company, 1974

2. Ito K: New Model Material for Photoelasticity and Photoplasticity, Experimental Mechanics, 1962, 2, (12)

3. Whitefield F. K. and Smith C. W.: Characterization Study of a Potential Photoplastic Material, Experimental Mechanics, 1972, 12, (2)

4. Dally J. W. and Mulc A.: Polycarbonate as a Model Material for Three Dimensional Photoplasticity, Trans. ASME, J. of Applied Mechanics, 95, Series E, 1973

5. Burger C. P.: Nonlinear Photomechanics, Experimental Mechanics, 1980, 20 (11)

6. Zhang, C. G, Jen, G. S., and Su, G. H.: Photoplastic simulation capability of domestic polycarbonate, J. of Ji-Lin Industrial University, 1988, (3)

7. Su. G. H.: Photoplastic study of planer swaging and wedge transverse deformation, degree thesis, Ji-Lin Industrial University, 1987

(continued on p.81)

DISTRIBUTION LIST

DISTRIBUTION DIRECT TO RECIPIENT

ORGANIZATION	MICROFICHE
B085 DIA/RTS-2FI	1
C509 BALL0C509 BALLISTIC RES LAB	1
C510 R&T LABS/AVEADCOM	1
C513 ARRADCOM	1
C535 AVRADCOM/TSARCOM	1
C539 TRASANA	1
Q592 FSTC	4
Q619 MSIC REDSTONE	1
Q008 NTIC	1
Q043 AFMIC-IS	1
E051 HQ USAF/INET	1
E404 AEDC/DOF	1
E408 AFWL	1
E410 ASDTC/IN	1
E411 ASD/FTD/TTIA	1
E429 SD/IND	1
P005 DOE/ISA/DDI	1
P050 CIA/OCR/ADD/SD	2
1051 AFIT/LDE	1
CCV	1
PO90 NSA/CDB	1
2206 FSL	1

Microfiche Nbr: FTD92C000289L
FTD-ID(RS)T-1065-91